

Application of Aperture Truncated Airy Beams in Free Space Optical Communications

Minghao Wang^{1,2}, Xiuhua Yuan¹, Peng Deng², Wei Yao³, Timothy Kane²

¹School of Optical and Electronic Information, Huazhong University of Science and Technology, Wuhan, China

²Department of Electrical Engineering, The Pennsylvania State University, University Park, USA

³Shenzhen Research Institute of Huazhong University of Science and Technology, Shenzhen, China.

e-mails: wmh@hust.edu.cn, yuanxh@hust.edu.cn, pxd18@psu.edu, weiyao@hust.edu.cn, tj7@psu.edu

Abstract—Free Space Optical Communications (FSOC) has proved to be a reliable alternative to radio frequency systems in providing high speed wireless data links, especially for satellite communications. To further improve the FSOC performance, plenty of novel light source beams are proposed and evaluated, among which Airy beams have gained intensive research efforts in the past decade, owing to its remarkable features. An ideal Airy beam is able to propagate in free space without diffraction, and it is resistant to atmospheric turbulence due to the self-healing feature. Besides, the main lobe of an Airy beam follows a controllable ballistic trajectory, which can be particularly useful to improve the link robustness in presence of blockage. However, if the transverse extent of the Airy beam is confined by a finite optical aperture, the non-diffractive features no longer retain. But within the limited diffraction-free range, the Airy beam is still able to self-heal and self-bend, making it valuable for enhancing the survivability of FSOC systems. In this study, we first examined the effects of truncation methods on the Airy diffraction-free range and found out that the aperture-truncated Airy (ati-Airy) beam is more preferable in terms of propagation distance. Then, the scintillation behavior of ati-Airy beams is investigated under the conditions of controlled self-bending as well as self-healing from obstructions.

Keywords—free space optical communications; Airy beam; truncated Airy beams; beam propagation; scintillation index.

I. INTRODUCTION

With the ever increasing demand of high bandwidth in satellite data transmission, in recent years Free Space Optical Communications (FSOC) has become one of the mainstream physical-layer technologies [1][2]. Most of the current FSOC systems use traditional Gaussian beams as the optical source. In order to improve the receiving performance, various novel beams have been proposed [3]-[6], among which is the Airy beam [7]. The reason why the Airy beam is considered promising in FSOC roots in its remarkable features—non-diffracting propagation in free space [8], self-accelerating in the transverse direction [9] and self-healing in the presence of obstacles [10].

In the context of FSOC, it is of great beneficial if optical beams can propagate without diffraction, since the power loss due to diffractive spreading can be minimized in long-haul links. However, for an Airy beam to fulfill the ideal diffraction-free feature, the transmitter (TX) optics should be

larger than the spatial extent of the Airy field, which is determined by $k^2 x_0^3$ [11], where k is the optical wave number and x_0 is the characteristic length of the Airy function. For effective capture and tracking in a practical system, x_0 should not be too small, and reasonable values of x_0 would require intimidatingly large TX apertures. That being said, in the real world of FSOC, the transmitting beam is always truncated by the finite TX aperture. Fortunately when that happens, the Airy beam is still able to propagate without much spreading within a limited distance called (nearly) diffraction-free range, beyond which severe diffraction takes place.

Despite its limited propagation distance, the truncated Airy beam is appealing. The well preserved self-accelerating feature makes it unique as an optical carrier, bringing the possibility of circumventing obstacles on the path to the receiver. If the obstacle is too big to circumvent, the Airy beam can even regenerate the blocked part of its optical field, which is known as self-healing. Therefore, optical links built with Airy beams can be more robust than the existing line-of-sight (LOS) links, especially in satellite communication scenarios, where blockage caused by clouds or other objects frequently occurs.

In this study we try to demonstrate the performance of truncated Airy beams in FSOC links. By means of wave optics simulation (WOS), the effects of various truncation methods on the diffraction-free range are numerically examined. Reaching at the conclusion that the aperture truncated ideal Airy beam is diffracted least, we further investigate its scintillation behavior when the ballistic trajectory is dynamically controlled. Then, by blocking the main lobe at the initial plane or at the halfway point of propagation, we have managed to analyze the aperture-averaged scintillation, as well as the mean Signal-to-Noise Ratio (SNR) of the regenerated main lobe. In addition to horizontal links, the propagation through vertically distributed turbulent atmosphere is also studied with non-uniformly distributed phase screens.

The rest of this paper is structured as follows. Section II is intended to find out in the presence of a circular hard aperture, which truncation method enables the longest diffraction-free propagation distance. Then, in Section III, the self-accelerating and self-healing properties of truncated Airy beams are examined from the perspective of scintillation index. Section IV is a brief summary of the presented work.

II. DIFFRACTION FREE RANGE OF TRUNCATED AIRY BEAMS

The Airy functions are the solution of the paraxial wave equation of diffraction, and for (1 + 1) D case the beam wave envelope is given as

$$U(s, \xi) = Ai(s - \xi^2 / 4) \exp[i(6s\xi - \xi^3) / 12], \quad (1)$$

where $s = x / x_0$ represents the transverse scale normalized by the Airy characteristic length x_0 , $\xi = z / kx_0^2$ is the normalized propagation distance, and $k = 2\pi/\lambda$ is the optical wavenumber.

In order to dynamically control the drop point, or the trajectory of the main lobe, the “initial velocity” parameter v is introduced into the initial plane expression which leads to

$$U(s, 0) = Ai(s) \exp[ivs], \quad (2)$$

from which the transverse shift of the main lobe s_0 can be determined by

$$s_0 = \xi^2 / 4 + v\xi. \quad (3)$$

Then, we can see that the acceleration of the ballistic is actually immutable (in the normalized s - ξ coordinate it is 1/2), yet the drop point of the main lobe can be easily controlled via v at a specified distance ξ .

Let us rewrite a 2D ideal Airy beam in the initial plane in this way:

$$U(s_x, s_y) = Ai(s_x) \exp[ivs_x] Ai(s_y) \exp[ivs_y], \quad (4)$$

where $s_x = x/x_0$ and $s_y = y/x_0$, with the characteristic length in both directions assumed to be equal.

As mentioned in the introduction, an ideal Airy beam exhibits infinite size and thus carries infinite energy, requiring truncation to restrict its power so that it can be physically realized. In the presence of truncation an Airy beam is no longer perfectly diffraction resistant. The specific truncation method matters a lot to its diffraction-free range.

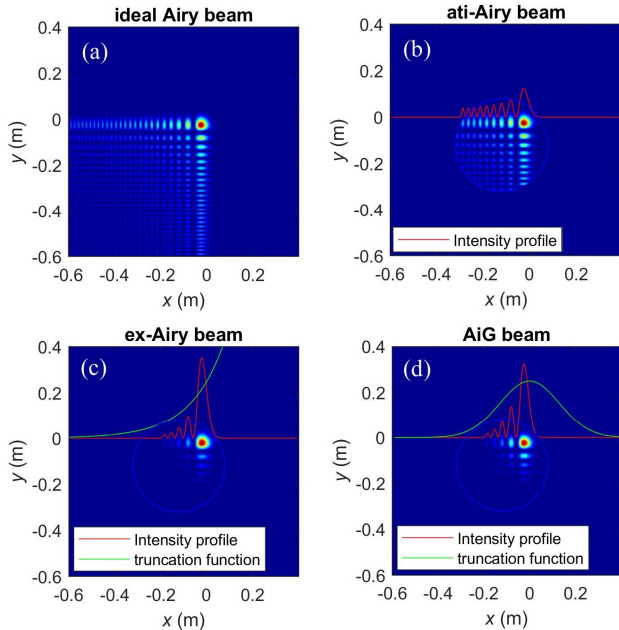


Figure 1. Intensity patterns at the initial plane of (a) ideal Airy beam without truncation, (b) aperture-truncated Airy beam, (c) exponentially decaying Airy beam and (d) Airy-Gauss beam.

In FSOC systems, the finite TX aperture forms a natural boundary, beyond which no beam wave field can exist. An ideal Airy beam truncated by the TX optics is called aperture-truncated ideal Airy (ati-Airy) beam, and its field in the initial plane can be written as

$$U_{\text{ati}}(s_x, s_y) = Ai(s_x) \exp(ivs_x) Ai(s_y) \exp(ivs_y) \times \text{circ}(R), \quad (5)$$

where $\text{circ}()$ is a circle binary window and R is the radius of the TX aperture.

Considering the rectangular shape of an Airy beam, to make full use of the circular aperture which is most common, we may not put the main lobe of the airy beam right in the center of the aperture. A feasible layout is illustrated in Figure 1 (a).

The most intensively studied finite energy Airy beam so far, however, is the exponentially decaying Airy (ex-Airy) beam, which in the initial plane can be expressed as

$$U_{\text{ex}}(s_x, s_y) = Ai(s_x) \exp[(\alpha + iv)s_x] Ai(s_y) \exp[(\alpha + iv)s_y], \quad (6)$$

where α is the exponential truncation factor, used to ensure spatial convergence of energy.

Another way to truncate an infinite Airy beam is to apply a Gaussian apodization, which is called the Airy-Gauss (AiG) beam:

$$U_{\text{AiG}}(s_x, s_y) = Ai(s_x) \exp[ivs_x] \times Ai(s_y) \exp[ivs_y] \exp[-r^2/\omega^2], \quad (7)$$

where $r = \sqrt{s_x^2 + s_y^2}$ and ω is the width of the Gaussian apodization function.

Since propagation distance is the major drawback of an FSOC system based on Airy beams, it is necessary to find out which truncation method in (5-7) enables the largest diffraction free range for a given TX aperture size and a constant Airy characteristic length. There is an analytic formula to calculate the non-diffraction range of an aperture truncated Airy beam [11], but there only the 1D case is considered and it is difficult to generalize to a 2D scenario where the Airy beam is truncated by a *circular* aperture. Also in [11], the authors have demonstrated that the expression for predicting the maximum propagation distance of ex-Airy beams in [12] is incorrect. As for the AiG beam, no prediction for the diffraction free range is available at all.

Here, we try to find out the maximum diffraction-free range of truncated Airy beams with characteristic length $x_0 = 25$ mm, and the TX pupil radius is set as $R = 200$ mm. In order to make a fair comparison between the three truncation methods, the truncation parameters of the ex-Airy beam and the AiG beam should be adjusted so that the presence or absence of the specific aperture barely causes extra power loss. This is important because aperture truncation exists anyway for any source beam. Further, the optical power of all the beams in the launching plane is made equal. With the above considerations, the launching fields within the aperture are shown in Figure 1 (b-d), where the intensity distribution of an ideal, untruncated Airy beam is also given as a reference in Figure 1 (a).

For more flexibility, we use the multi-step wave optics simulation (WOS), which is a numerical method based on the FFT version of the Fresnel diffraction integral [13], to

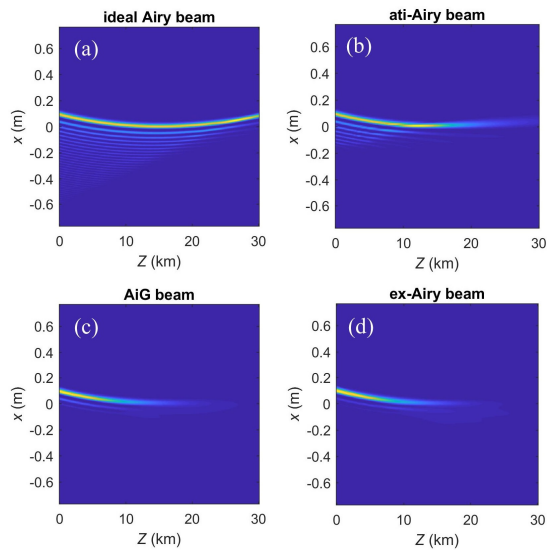


Figure 2. Evolution of intensity profiles in the x - z plane of (a) ideal Airy beam without truncation, (b) aperture-truncated Airy beam, (c) exponentially decaying Airy beam and (d) Airy-Gauss beam.

simulate the propagation process of those truncated Airy beams. Here, the diffraction free range is defined as the distance from the initial plane at which the full width at half maximum (FWHM) of the intensity peak of the main lobe doubles. And the FWHM of the main lobe is measured by its width on the diagonal of the quadrature Airy pattern. The evolution of intensity cross-section of the four Airy beams from Figure 1 is shown in Figure 2, and the corresponding measured FWHMs are given in Figure 3. It is clearly seen that apart from the ideal Airy beam, all the truncated beams are subjected to diffractive spreading beyond a certain distance. In comparison with the ex-Airy beam and the AiG beam, the ati-Airy beam has an obviously longer range of nearly diffraction-free propagation, which is about 27 km in this case, well consistent with the conclusion drawn in [11]. The other two counterparts, however, rapidly collapse beyond 18 km, and are thus excluded from further discussions below.

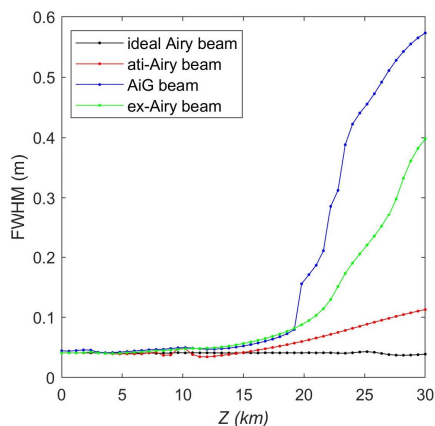


Figure 3. FWHM as a function of propagation distance of Airy beams with different truncations.

III. EFFECTS OF SELF-ACCELERATION AND SELF-HEALING ON SCINTILLATION IN ATMOSPHERIC TURBULENCE

In Section II, we have made it clear that in terms of propagation distance, the ati-Airy beam performs better as an optical carrier than the ex-Airy beam and the AiG beam. And in this section we will find out how well ati-Airy beam's self-acceleration and self-healing act in turbulent atmosphere.

A. Self-acceleration

Without external refractive-index potential along the whole optical path, the acceleration of lateral shift of an Airy beam is only dependent on the Airy characteristic length x_0 . If x_0 is constant then in a specified meridian plane, there is only one possible initial velocity/launching angle for the main lobe to connect the transmitter with a certain receiver. But since in the 3D space there are numerous meridian planes, circumvents are possible if we just rotate the 2D launching beam pattern in the launching plane. Under conditions that the transceivers suffer from vibrations, dynamically controlled drop points can be useful in fast tracking.

Now, we are interested in that whether the dynamic control of the ballistic trajectory would affect the turbulence reception performance. To this end, we will examine the scintillation index of an ati-Airy beam in a 20 km horizontal link. The transmitting beam is the ati-Airy beam shown in Figure 1(b), with $x_0 = 25$ mm, and its main lobe adjusted to (0.1 m, 0.1 m) position in the launching plane to fully utilize the aperture with radius $R = 200$ mm. The drop point of the main lobe is controlled by v through (3), ranging from $x \in (0, 0.5$ m) in the receiver plane, and the free-space trajectories of the main lobe are plotted in Figure 4(a). The atmospheric channel is implemented through 17 evenly distributed phase screens, sampled by 512 points with 3 mm sampling intervals in each side. The scintillation is calculated by the normalized intensity flux variance of a $D = 20$ mm receiver centered on the main lobe intensity peak, and the results are shown in Figure 4(b). The minor fluctuations in the curve are mainly due to simulation inaccuracies, and it is safe to conclude that for truncated Airy beams, the scintillation behavior is not affected by the initial velocity control.

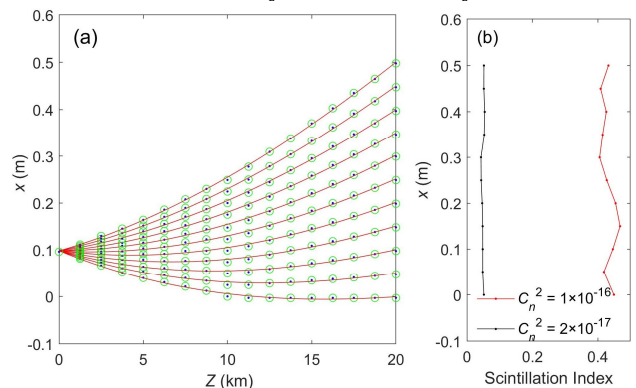


Figure 4. Ati-Airy beams with varied initial velocities. (a) trajectories of the main lobe and (b) scintillation measured at the drop point on the receiver plane.

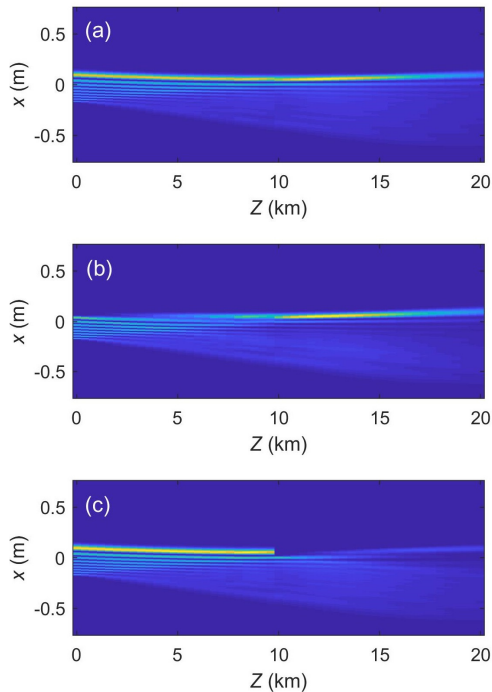


Figure 5. Evolution of intensity profiles of an anti-Airy beam (a) without obstruction, (b) with the main lobe obstructed at the initial plane and (c) with the main lobe obstructed at 10 km.

B. Self-healing

Then we look into the self-healing of anti-Airy beams. Figure 5 illustrates the self-healing process of anti-Airy beams. Figure 5(a) shows an unobstructed anti-Airy beam propagating in free space, while in Figure 5(b) the main lobe is obstructed in the initial plane, and in Figure 5(c) the obstruction is applied in the middle of the path, i.e. 10 km. We see that when the main lobe is obstructed in the initial plane, it is almost fully recovered at the receiver end. By comparison, if the obstruction happens halfway, the recovered main lobe seems much weaker in intensity. One reason for this is because in halfway the side lobes have already dispersed and thus are not able to provide as much power flow. The other reason is that the recovery distance in the case of Figure 5(c) is shorter than that in Figure 5(b). Anyway, in either case the receiver, located at the position where the main lobe is supposed to be, is able to detect the recovered signal so that the link will not fail.

Next, we study the scintillation behavior of the anti-Airy beams with obstructions located at positions as shown in Figure 5(b, c). Nevertheless considering the fact that not all obstacles are totally opaque, we introduce the transparency of the obstacle as a variable τ , and the shape of the obstacle is a rectangle that just covers the main lobe of the Airy beam, see Figure 6 for the effect and shape of the obstacle in the initial plane.

We will begin with a 20 km horizontal link then a 20 km vertical link. The horizontal atmospheric link parameters for simulation are the same as those used in Figure 4(b), only that

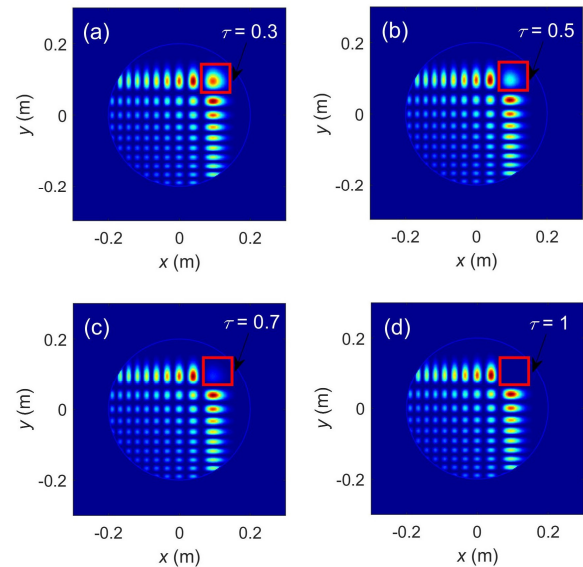


Figure 6. Shape and effect of the obstacle at the launching plane with transparency (a) $\tau = 0.3$, (b) $\tau = 0.5$, (c) $\tau = 0.7$ and (d) $\tau = 1$.

the lateral shift is set to be zero. Three different receiver (RX) aperture sizes are considered, namely, 20 mm, 50 mm, and 100 mm, all centered at the intensity peak of the receiving main lobe. Simulation results are shown in Figure 7.

It seems neither the scintillation behavior nor the mean SNR is greatly affected, indicating that the self-healing process has perfectly counteracted the effects of the obstacle obstructing the main lobe in the launching plane. Similar results can be seen in Figure 8 in which case the main lobe is obstructed at 10 km, i.e. halfway of the path.

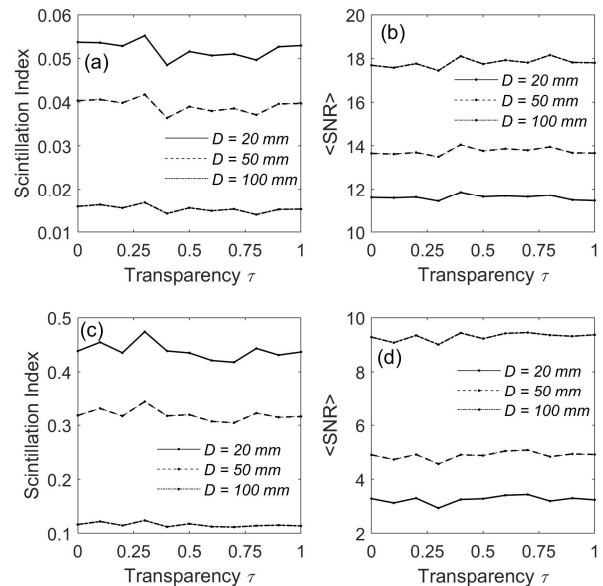


Figure 7. With the main lobe obstructed in the launching plane, aperture-averaged scintillation and mean SNR of anti-Airy beams as a function of the obstacle transparency τ in a 20 km horizontal link with (a, b) $C_n^2 = 2 \times 10^{-17}$ and (c, d) $C_n^2 = 1 \times 10^{-17}$.

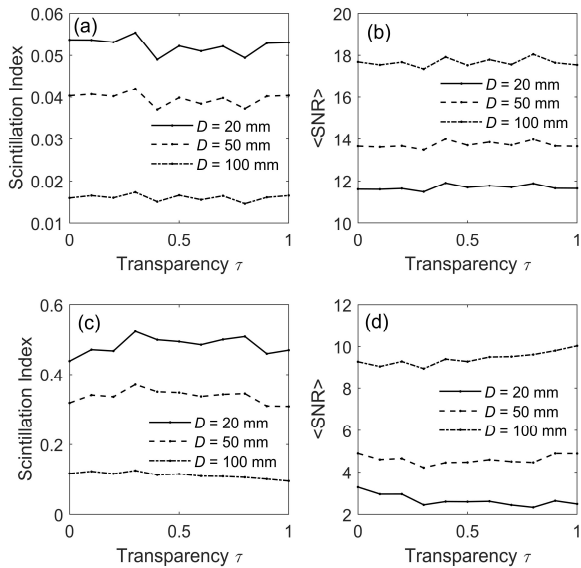


Figure 8. With the main lobe obstructed at 10 km, aperture-averaged scintillation and mean SNR of ati-Airy beams as a function of the obstacle transparency τ in a 20 km horizontal link with (a, b) $C_n^2 = 2 \times 10^{-17}$ and (c, d) $C_n^2 = 1 \times 10^{-17}$.

Until now we have investigated Airy beams propagating along a horizontal path. Taking advantage of the flexibility of wave optics simulation, we can further examine the performance of Airy beams in turbulent vertical paths. We simulated the case of a 20 km vertical turbulence channel where the H-V_{5,7} model [14] is applied with the ground-level turbulence set to $C_n^2(0) = 1 \times 10^{-14}$. To account for the altitude dependent C_n^2 profile, 17 nonuniformly distributed turbulence phase screens are used for accurate simulation of the channel. The obstacle is put at the halfway of the path, i.e. 10 km, obstructing the main lobe. The results are shown in Figure 9, from which we can see that in the uplink, if the obstacle is translucent then the scintillation will increase a bit but if it is totally opaque, the scintillation even decreases compared with the case of no obstacle ($\tau = 0$), and the resultant mean SNR can increase by 1 dB. While for the downlink, highly opaque obstacles will lead to increase scintillation and decreased SNR.

In general, the self-healing of the ati-Airy beam makes it resistant to obstructions in its propagation path, as a result of which the reception performance is not heavily degraded. This can be explained this way: when the main lobe is blocked, the power of the adjacent side lobes begins to flow to the vacancy. Note that this self-healing flow of optical power comes from a larger area than that occupied by the original main lobe, giving rise to some area averaging in scintillation. This type of averaging also takes place in the propagation of self-focusing beams, such as RPCBs (Radial Partially Coherent Beams) [15], working in essentially the same mechanism with the well-known aperture averaging effect.

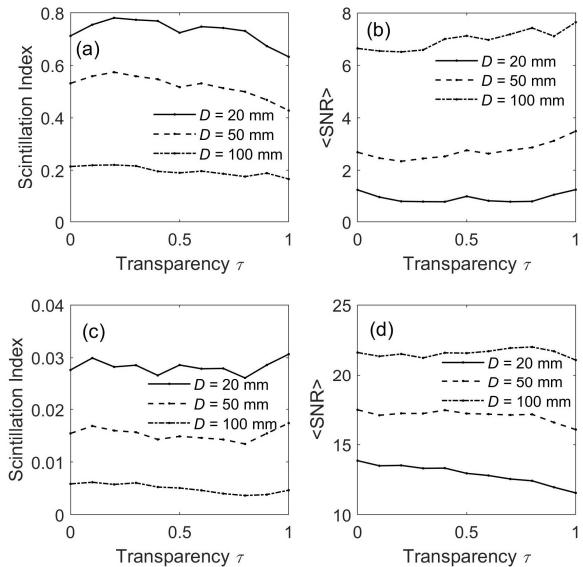


Figure 9. With the main lobe obstructed at 10 km, aperture-averaged scintillation and mean SNR of ati-Airy beams as a function of the obstacle transparency τ in a 20 km (a, b) uplink and (c, d) downlink.

As can be seen from the results in this section, the self-acceleration and self-healing of truncated Airy beams are barely affected by the presence of turbulence. Therefore, these beneficial properties can be exploited in atmospheric free-space laser communication channels.

IV. CONCLUSION AND FUTURE WORK

To investigate the feasibility of applying Airy beams in FSOC systems, we have firstly compared the diffraction-free range of three commonly used truncated Airy beams. With the presence of a hard aperture, an ideal Airy beam with no additional truncation (i.e., the ati-Airy beam) can propagate longer than the exponentially decaying Airy beam and the Airy-Gauss beam, making it more preferable for long-distance FSOC links. Then, the scintillation behavior of ati-Airy beams is studied when the lateral shift acceleration is controlled. It is found that varying the initial velocity will not obviously affect the reception quality. Moreover, the area scintillation and mean SNR of ati-Airy beams in the presence of an obstacle with varying transparency is examined. According to the simulation results, if either the main lobe of the beam is obstructed in the launching plane or in halfway, either in a horizontal or a vertical path, the reception performance maintains quite well. This strongly indicates that, the self-healing feature of an ati-Airy beam makes it resistant to obstacles blocking the propagation path and can thus benefit the link robustness a lot.

In the following research, we will investigate the feasibility of applying truncated symmetrical Airy beams in long distance free-space laser communications.

REFERENCES

- [1] L. C. Andrews and R. L. Philips, *Laser Beam Propagation Through Random Media*, 2nd ed, SPIE, Bellingham, WA, 2005.

- [2] C. C. Murat Uysal, Z. Ghassemlooy, A. Boucouvalas, E. Udvary (Eds.), *Optical Wireless Communications - An Emerging Technology*, Springer International Publishing, Switzerland, 2016.
- [3] X. Ji, H. Chen, and G. Ji, "Characteristics of annular beams propagating through atmospheric turbulence along a downlink path and an uplink path," *Appl. Phys. B*, vol. 122, pp. 221, 2016.
- [4] I. Ituen, P. Birch, C. Chatwin, and R. Young, "Propagation of Bessel beam for ground-to-space applications," in *Propagation through and Characterization of Distributed Volume Turbulence and Atmospheric Phenomena*, Optical Society of America, 2015, PM3C. 4.
- [5] G. Gbur, "Partially coherent beam propagation in atmospheric turbulence [Invited]," *J. Opt. Soc. Am. A*, vol. 31, pp. 2038-2045, 2014.
- [6] M. Wang, X. Yuan, J. Li, and X. Zhou, "Radial partially coherent beams for free-space optical communications," in *Laser Communication and Propagation through the Atmosphere and Oceans VI*, International Society for Optics and Photonics, 2017, pp. 1040813.
- [7] G. A. Siviloglou and D. N. Christodoulides, "Accelerating finite energy Airy beams," *Opt. Lett.*, vol. 32, pp. 979-981, 2007.
- [8] Y. Hu, G. A. Siviloglou, P. Zhang, N. K. Efremidis, D. N. Christodoulides, and Z. Chen, "Self-accelerating Airy Beams: Generation, Control, and Applications," *Springer* 170, pp. 1-46, 2012.
- [9] G. A. Siviloglou, J. Broky, A. Dogariu, and D. N. Christodoulides, "Ballistic dynamics of Airy beams," *Opt. Lett.*, vol. 33, pp. 207-209, 2008.
- [10] J. Broky, G. A. Siviloglou, A. Dogariu, and D. N. Christodoulides, "Self-healing properties of optical Airy beams," *Opt. Express*, vol. 16, pp. 12880-12891, 2008.
- [11] X. Chu, S. Zhao, and Y. Fang, "Maximum nondiffracting propagation distance of aperture-truncated Airy beams," *Opt. Commun.*, vol. 414, pp. 5-9, 2018.
- [12] J. Rogel-Salazar, H. Jiménez-Romero, and S. Chávez-Cerda, "Full characterization of Airy beams under physical principles," *Phys. Rev. A*, vol. 89 (2), pp. 023807, 2014.
- [13] D. G. Voelz, *Computational Fourier Optics: A MATLAB Tutorial*, SPIE Press, Bellingham, Washington, USA, 2011.
- [14] R. R. Beland, "Propagation through atmospheric optical turbulence," *Atmospheric Propagation of Radiation*, vol. 2, pp. 157-232, 1993.
- [15] M. Wang, X. Yuan, and D. Ma, "Potentials of radial partially coherent beams in free-space optical communication: a numerical investigation," *Appl. Opt.*, vol. 56, pp. 2851-2857 2017.